Broken Symmetry States around *Tunable* Van Hove Singularity in Moire Band

Liang Fu

KITP, Santa Barbara, 1/17/2019

Collaboration

Noah Yuan

Hiroki Isobe

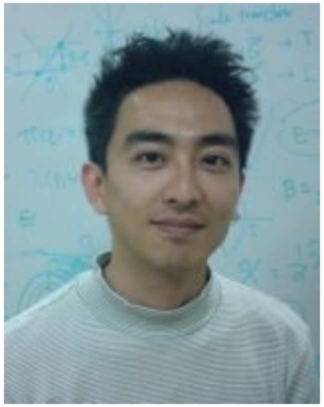

Mikito Koshino (Osaka)

and Zheng Zhu & Donna Sheng (CSUN)

Outline

- Narrow moire band and van Hove singularity
- Unconventional SC and density wave near VHS
- Tuning to **magic VHS**
- Effective tight-binding/Hubbard model

Magic-Angle Twisted Bilayer Graphene

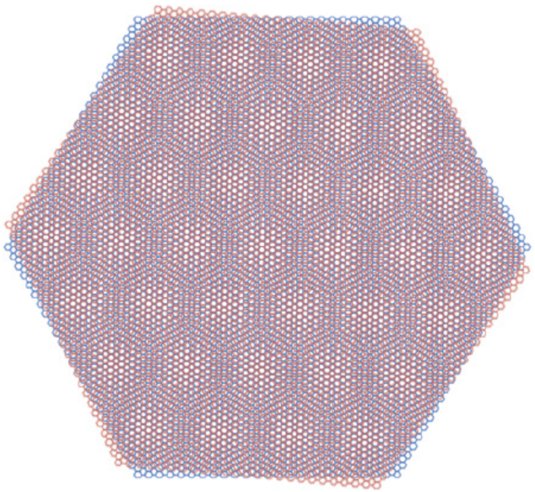

At θ~1°: 10,000 atoms per moire cell

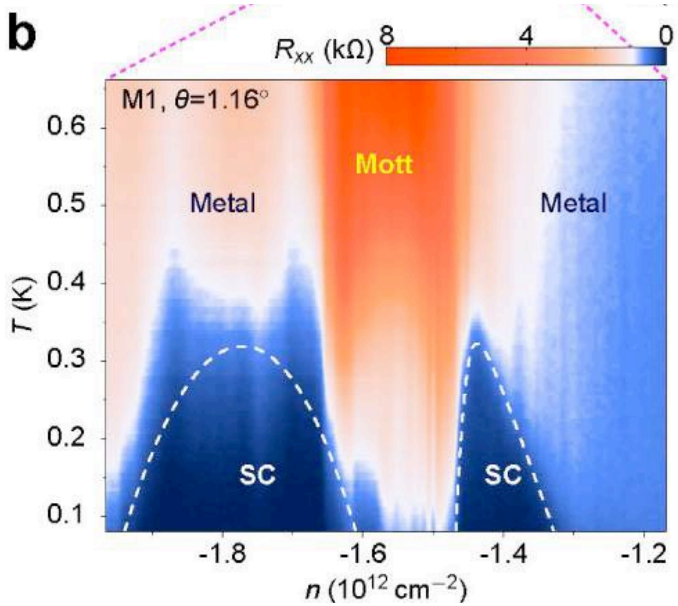

Doping turns conductor into insulator and SC

Cao et al, Nature **556**, 80 (2018)

Hierarchy of Scales

Spanning 4 orders of magnitude in energy:

Graphene	1eV	Dirac fermions
Twisted Bilayer Graphene	100meV	Interlayer coupling
Narrow Band at magic angle	10meV	Van Hove singularity
Insulator & Superconductor	1K	SC gap

Continuum Model

Band structure of TBG modeled by interlayer coupling of Dirac fermions

- Dirac velocity: v
- Twist angle: θ
- Interlayer hopping:

$$u_{AA} = u_{BB} \equiv u,$$
$$u_{AB} = u_{BA} \equiv u'$$

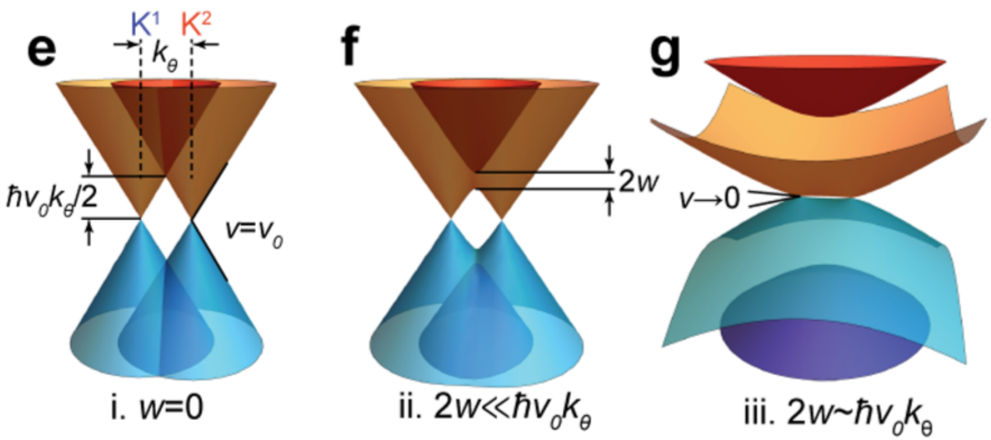

For non-relaxed bilayer structures, **u=u’**

Inter-valley scattering between K and K’ is suppressed at small twist angle

Flat band at magic angle ~ 1

Bistritzer & MacDonald (2011)

Lattice Relaxation

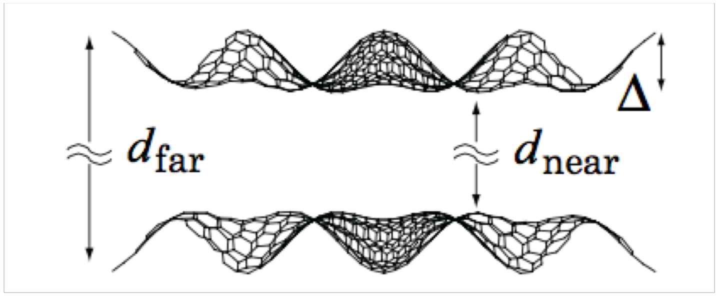

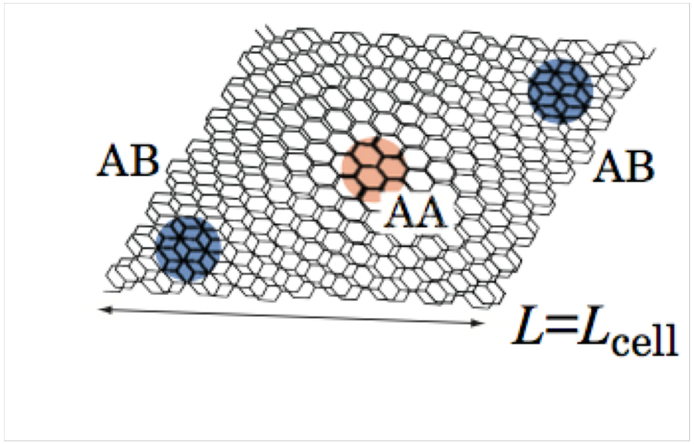

Uchida et al., PRB 90, 155451 (2014)

Generalized Continuum Model

Koshino, Yuan, Koretsune, Ochi, Kuroki & LF, Phys. Rev. X (2018)

θ=1.05°

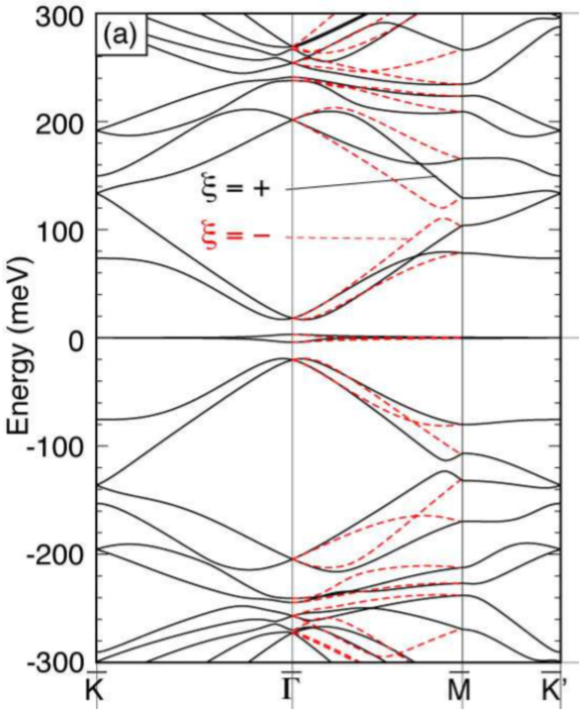

due to lattice distortion

$$u_{AA} = u_{BB} < u_{AB} = u_{BA}$$
$$u = 79.7\text{meV}, \qquad u' = 97.5\text{mev}$$

4 moire bands from 2 valleys & 2 sublattices:

- bandwidth ~ 10meV,
- gap to higher bands ~ 15meV (transport gap: 40meV)

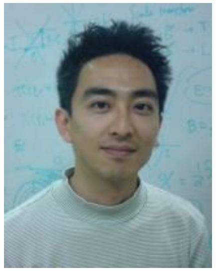

In-plane relaxation: Nam & Koshino (2017)

Full relaxation Carr, Fang, Zhu & Kaxiras (2019)

Separation of Scales

4 orders of magnitude in energy:

Graphene	1eV	Dirac fermions
Twisted Bilayer Graphene	100meV	Interlayer coupling
Narrow Band at magic angle	10meV	Van Hove singularity
Insulator & Superconductor	1K	SC gap

Normal State inside Narrow Band

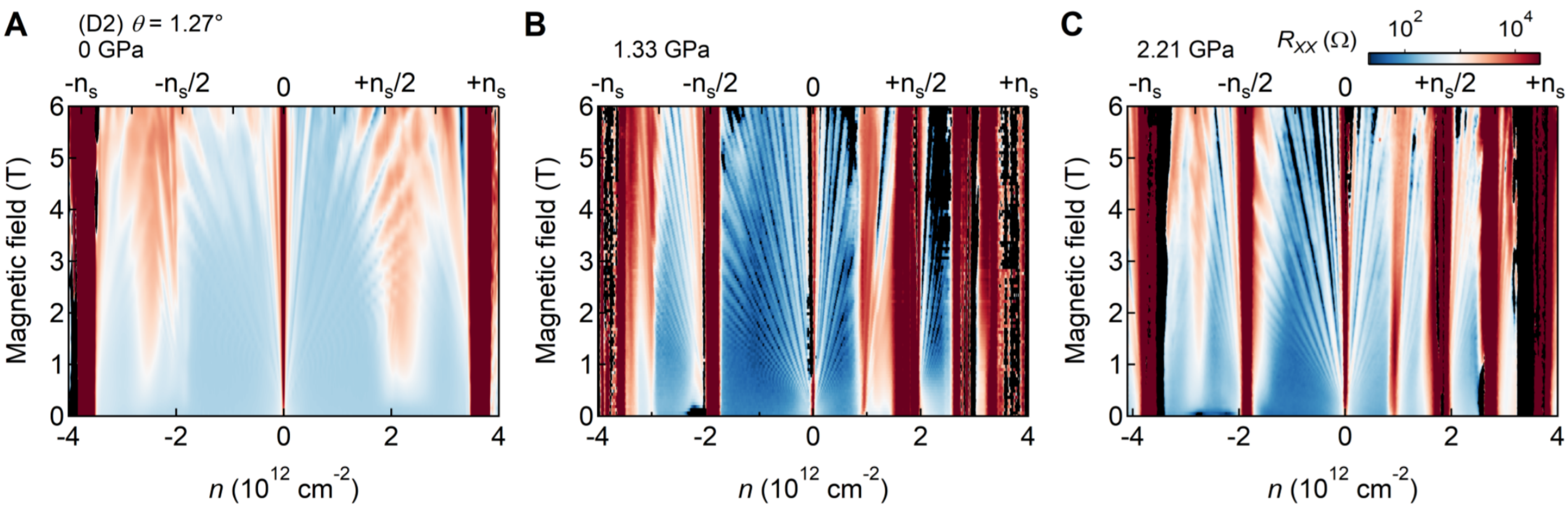

Well-defined Fermi surface in a wide doping range

Bandwidth comparable to Interaction

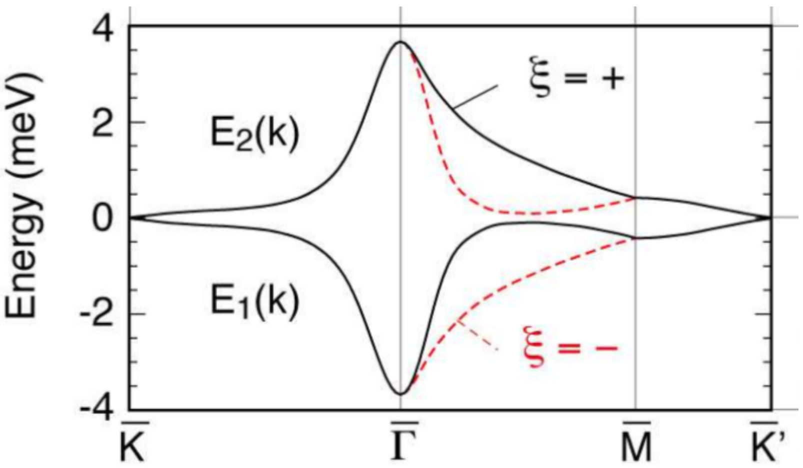

- Two valleys related by time-reversal: $E_{+}(k) = E_{-}(-k)$
- Absence of inversion within a valley: $E_{+}(k) \neq E_{+}(-k)$

Recent STM data show moire bandwidth is **a few tens of meV**, possibly due to many-body enhancement of Dirac velocity in graphene

Coulomb interaction: $$\frac{e^2}{\epsilon\lambda} \simeq \frac{100\text{meV}}{\epsilon}$$

ϵ accounts for screening from substrate and <u>higher bands</u>

U/t is of order one

Fermi Contour and Van-Hove Singularity

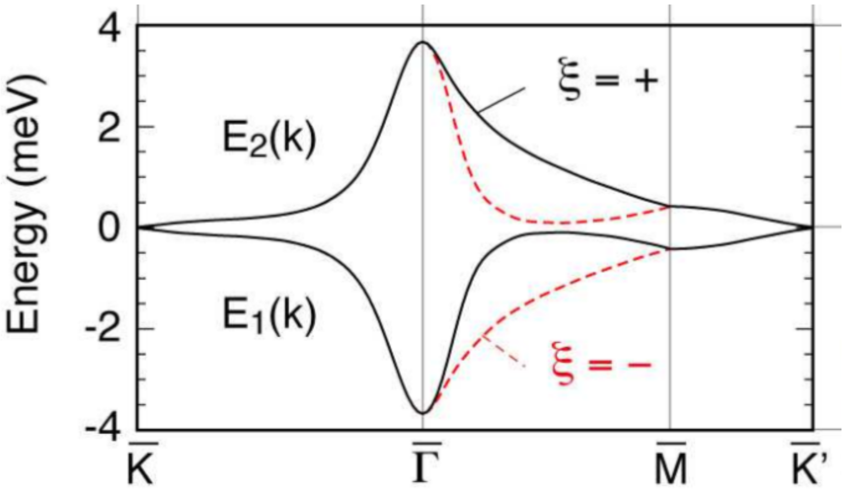

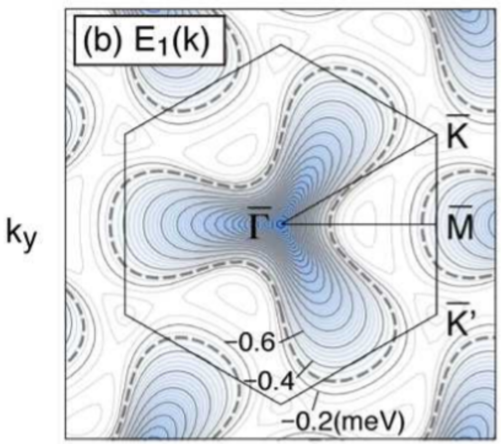

- Under doping, disjoint Fermi pockets around Dirac points evolve into single pocket around Γ, resulting electron-hole conversion

van-Hove singularity at Lifshitz transition

Charge Inversion and Topological Phase Transition at a Twist Angle Induced van Hove Singularity of Bilayer Graphene

Youngwook Kim,[†] Patrick Herlinger,[†] Pilkyung Moon,[‡,§] Mikito Koshino,[∥] Takashi Taniguchi,[⊥] Kenji Watanabe,[⊥] and Jurgen H. Smet[*,†]

Nano Letter (2016)

R_{xy} θ=1.8

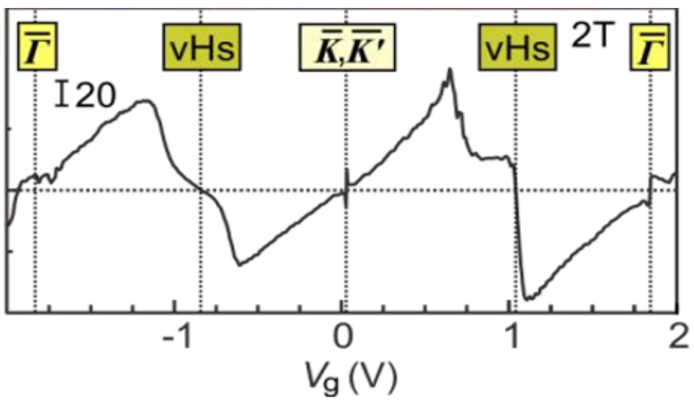

see also Cao et al, PRL (2016)

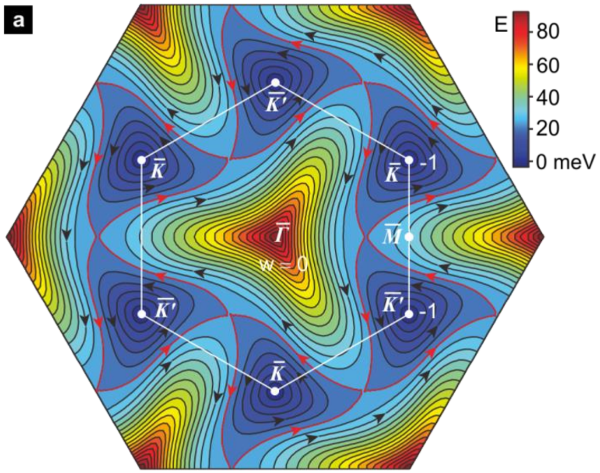

Hall changes sign close to n_s=2: Van Hove singularity close to Fermi level

Van Hove Singularity seen in STM

θ=1.79

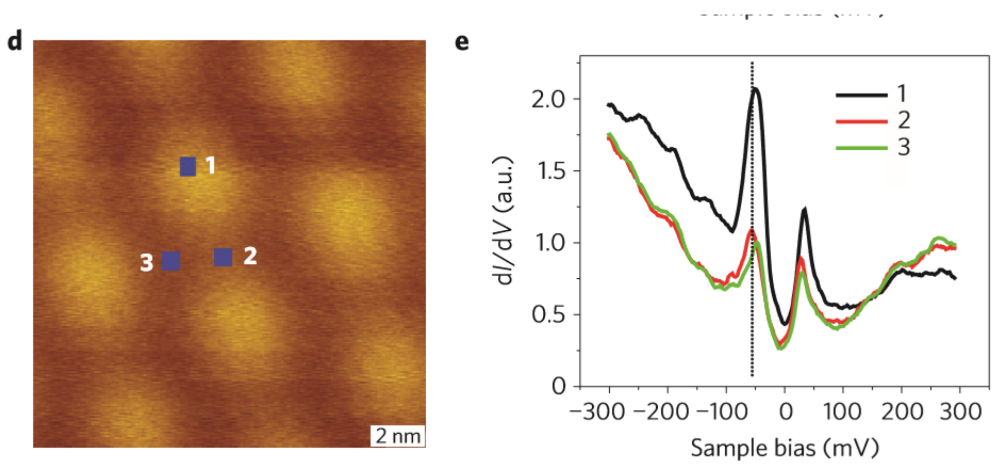

θ=1.16

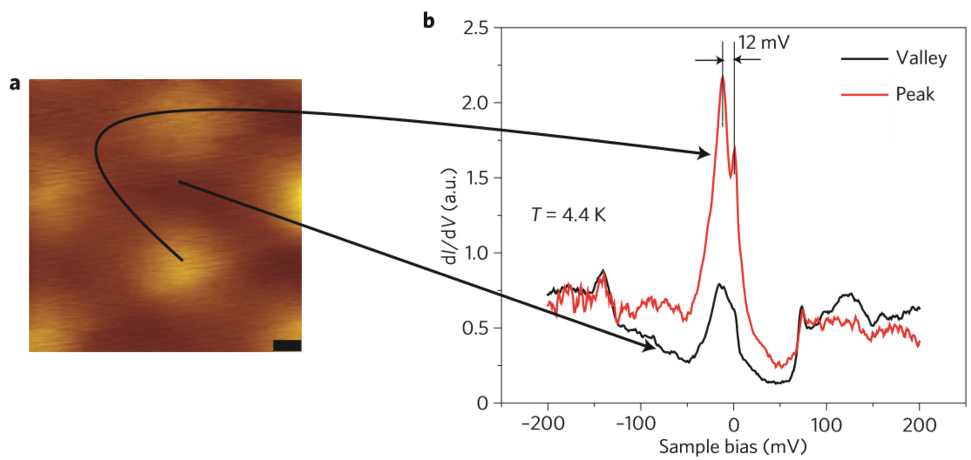

Eva Andrei et al, Nat Phys (2010) (CVD-grown & graphene on graphite)

Van Hove Physics

Quantum **criticality** due to **topological transition** of Fermi surface:

Diverging DOS leads to strong tendency to various competing/intertwined broken symmetry states:

- ferromagnetism, nematicity
- superconductivity
- charge/spin density wave

$$\chi = \frac{\chi_0}{1 - \chi_0 U}, \qquad \chi_0 \propto \rho$$

Van Hove Physics

Quantum **criticality** due to **topological transition** of Fermi surface:

Diverging DOS leads to strong tendency to various competing/intertwined broken symmetry states:

- ferromagnetism, nematicity
- superconductivity
- charge/spin density wave

$$\chi = \frac{\chi_0}{1 - \chi_0 U}, \qquad \chi_0 \propto \rho$$

Long history: cuprates, ruthenates, monolayer graphene …

Chiral superconductivity from repulsive interactions in doped graphene

Rahul Nandkishore[1], L. S. Levitov[1] and A. V. Chubukov[2]*

2D moire materials offer an unprecedented and ideal platform to access van Hove filling by gating without introducing disorder

Van Hove Hot Spot & Fermi Surface Nesting

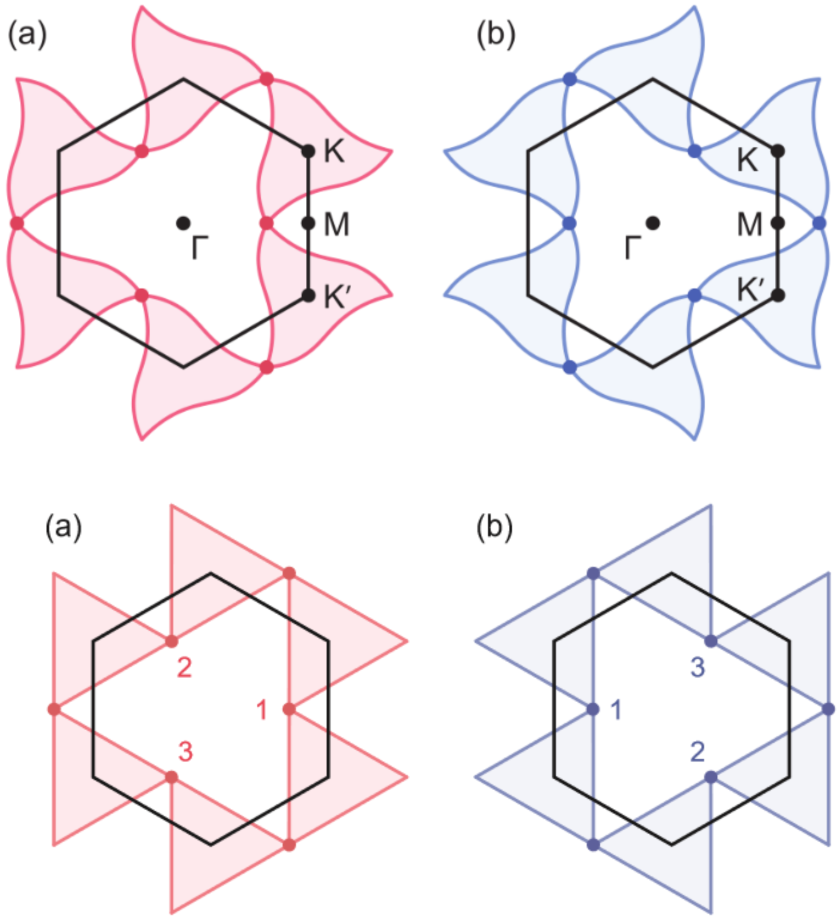

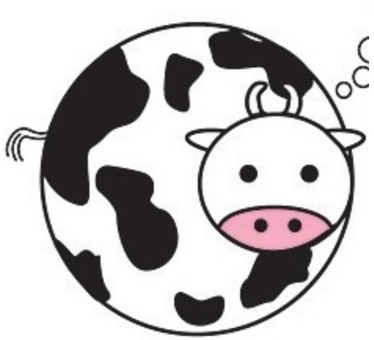

Isobe, Yuan & LF, Phys. Rev. X (2018)

Van Hove Hot Spot & Fermi Surface Nesting

Our Model:

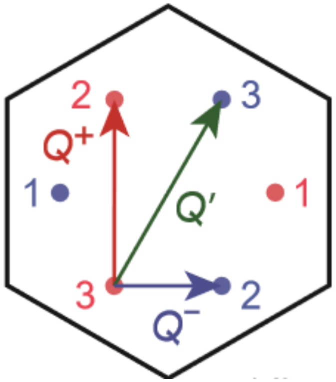

- 6 hot spots related by symmetry
- Good nesting of inter-valley density wave at Q' and Q-

Under this condition, SC and density waves have largest bare susceptibility, hence compete.

Isobe, Yuan & LF, Phys. Rev. X (2018)

Electron Interaction

Two types of scattering processes among hot spots:

- Density interaction from long-range Coulomb interaction
- Inter-valley exchange interaction from short-range interaction => small at low density

Density interactions

$n_\tau n_\tau$ ($\tau = \pm$: valley) $\quad n_+ n_-$

Inter-valley exchange interactions

$c^+_{+\alpha} c_{-\alpha} c^+_{-\beta} c_{+\beta}$ (α, β: spin)

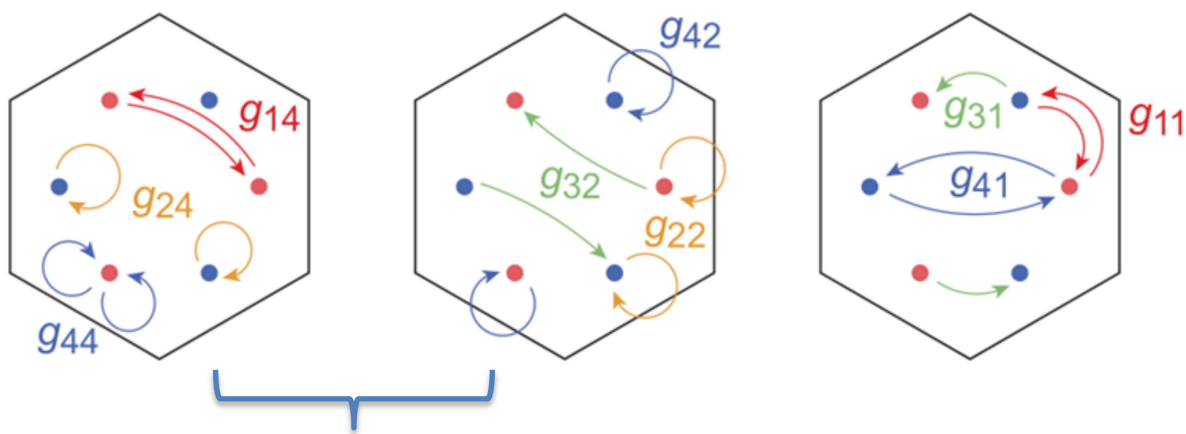

U(2)*U(2)

U(2)

RG equation

Coupled RG equations for coupling constants

$$\dot{g}_{14} = \dot{g}_{24} = \dot{g}_{44} = 0,$$
$$\dot{g}_{22} = -d_{3-}(g_{11}^2 + g_{22}^2) + d_{1-}(g_{22}^2 + g_{32}^2),$$
$$\dot{g}_{32} = -(g_{31}^2 + g_{32}^2 + 2g_{31}g_{41} + 2g_{32}g_{42}) + 2d_{1-}g_{22}g_{32},$$
$$\dot{g}_{42} = -(2g_{31}^2 + 2g_{32}^2 + g_{41}^2 + g_{42}^2) + d_{2-}g_{42}^2,$$
$$\dot{g}_{11} = -2d_{3-}g_{11}g_{22} + 2d_{1-}(g_{11}g_{22} - g_{11}^2 + g_{31}g_{32} - g_{31}^2),$$
$$\dot{g}_{31} = -2(g_{31}g_{32} + g_{31}g_{42} + g_{32}g_{41}) + 2d_{1-}(g_{11}g_{32} + g_{22}g_{31} - 2g_{11}g_{31}),$$
$$\dot{g}_{41} = -2(2g_{31}g_{32} + g_{41}g_{42}) + 2d_{2-}(g_{41}g_{42} - g_{41}^2)$$

d: nesting parameters

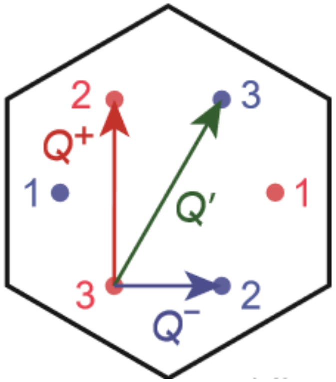

- Attraction in BCS channel grows
- Repulsion in nesting channel grows

RG Flow

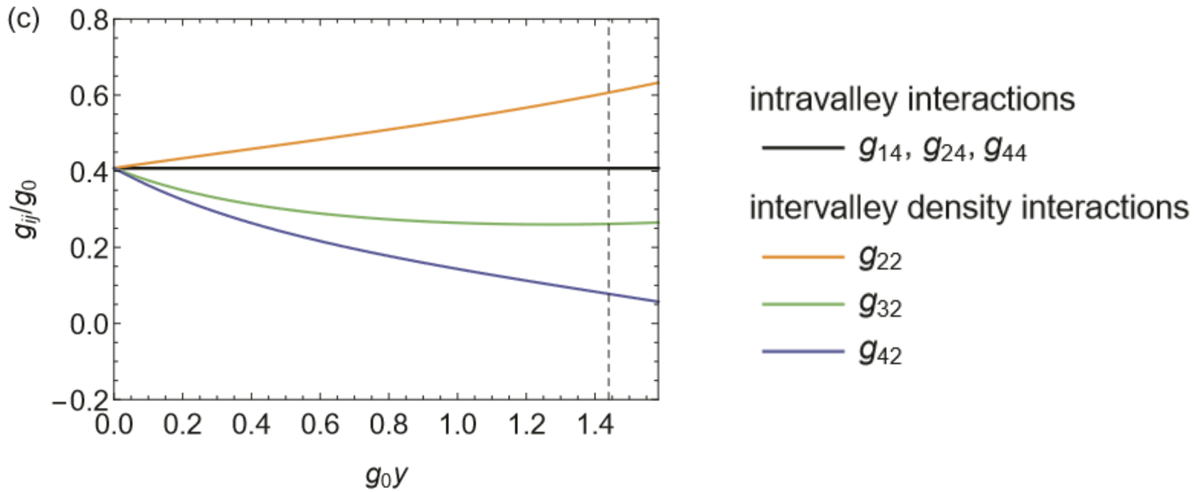

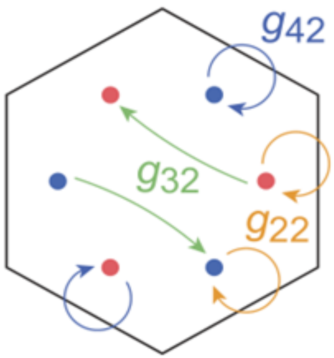

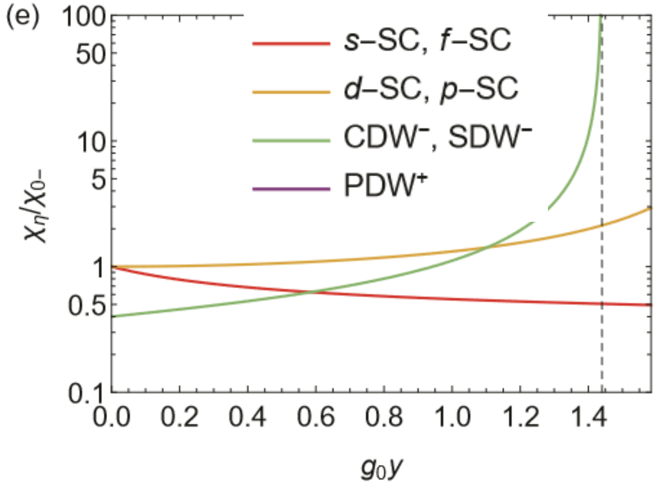

- Strong nesting:
  charge or spin density-wave states at Q^-
- Weak nesting:
  d-wave spin-singlet or p-wave spin-triplet SC
  (attraction is generated from bare repulsion)

Degeneracy within density wave or within SC is lifted by small inter-valley exchange interaction.

Energy Spectrum of Density Wave at $Q^{-} = \Gamma M/2$

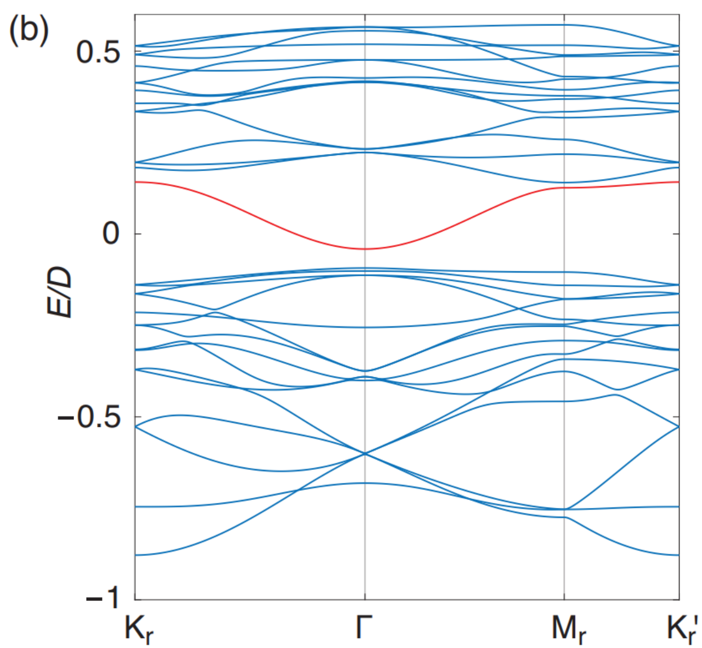

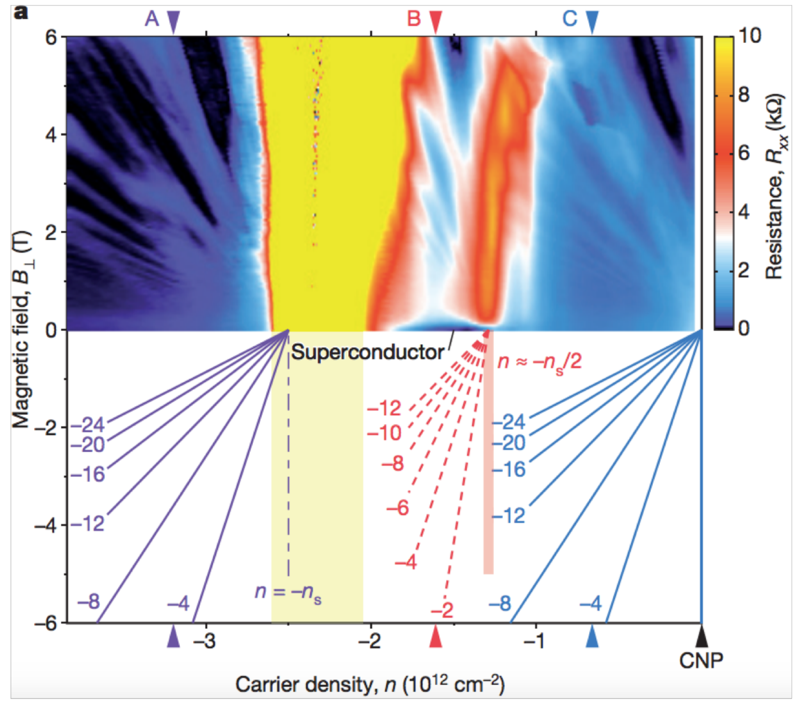

Period-4 density wave at half filling (n_s=2):

- Direct gap at Γ point => correlated insulator
- Single pocket (with spin degeneracy) above the gap; two heavy pockets below the gap

Isobe, Yuan & LF, Phys. Rev. X (2018)

Relationship of SC and Density Wave

Doping controls Fermi surface nesting & commensuration:

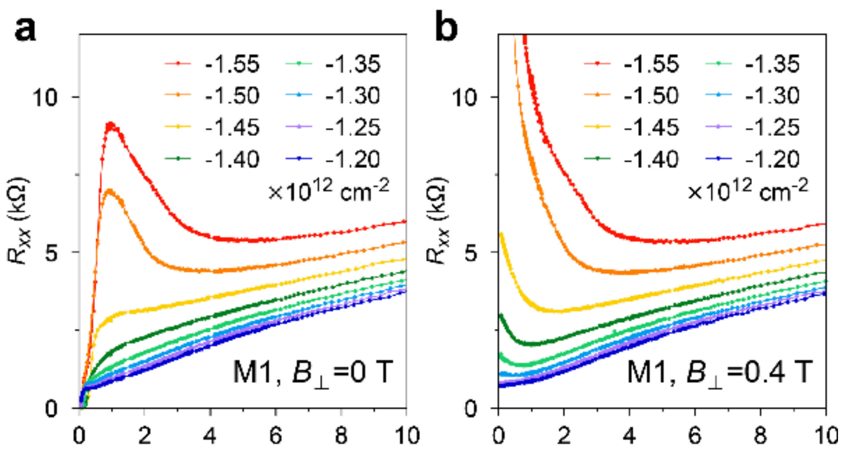

In our model, SC and density wave are driven by the same interaction, which grows at low temperature due to Fermi surface nesting. Which phase is realized depends on FS condition and commensuration.

- At half filling, Umklapp scattering stabilizes commensurate density wave
- Two-component SC order parameter => chiral and nematic SC

Related works: Xu, Balents (PRL 2018); Kennes, Lischner, Karrasch (PRB 2018); You, Vishwanath (arXiv, 2018); Wu, Pawlak, Jian, Xu (arXiv, 2018); Padhi, Setty, Phillips (Nano Lett 2018); Venderbos & Fernandes (PRB 2018)…

VHS at Magic Angle

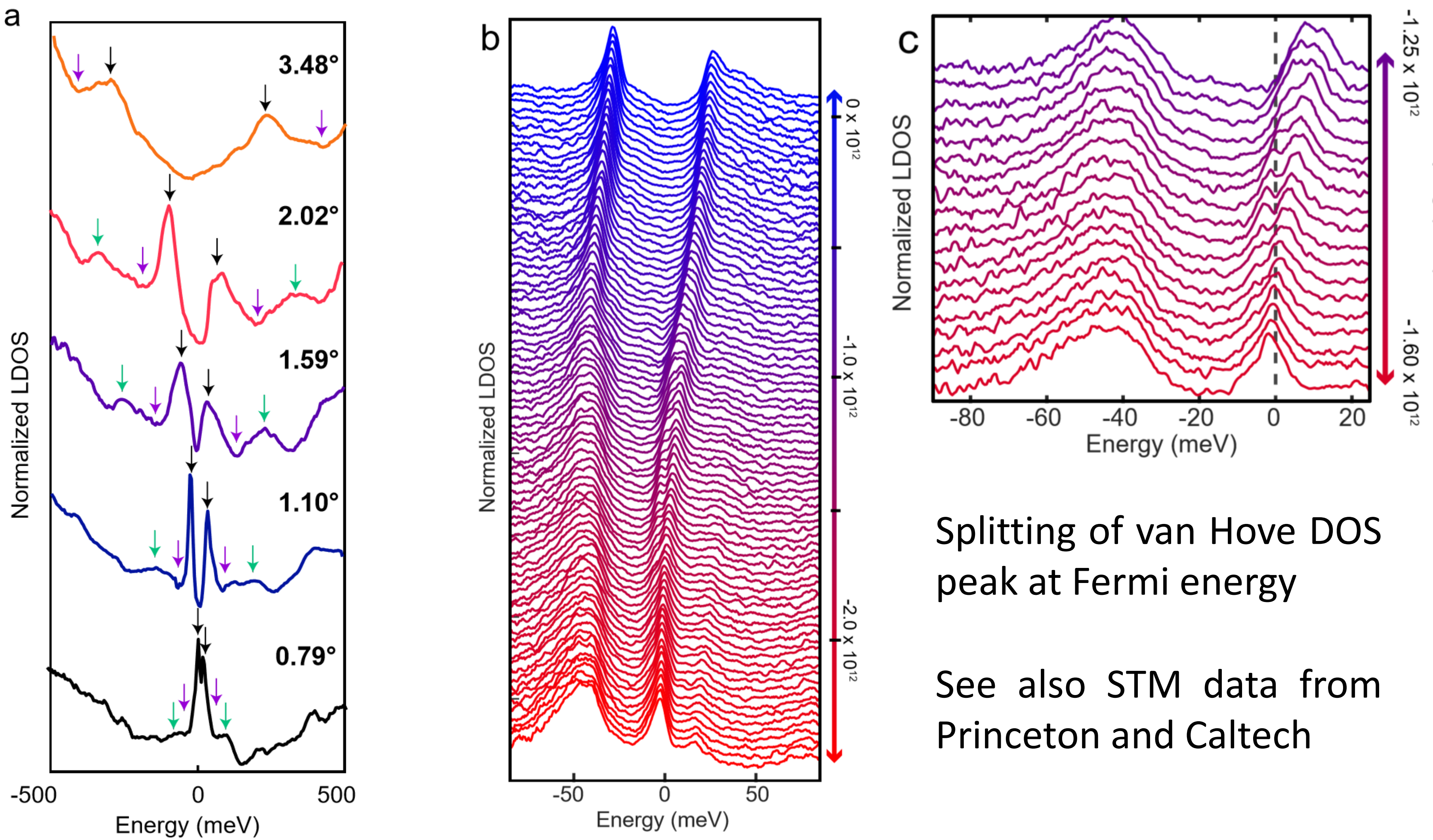

Splitting of van Hove DOS peak at Fermi energy

See also STM data from Princeton and Caltech

Pasupathy & Dean, arXiv:1812.08776

Two VHS Configurations

θ=1.8

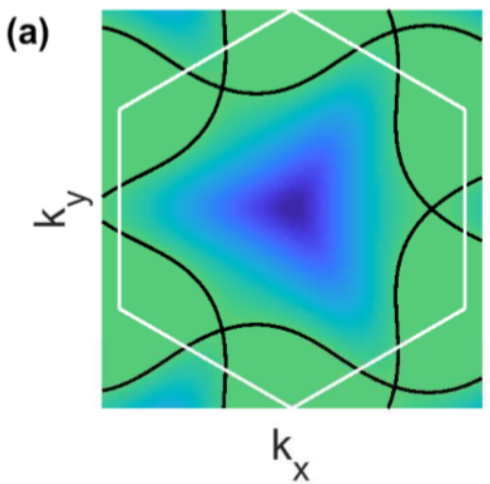

- 3 VHS on ΓM line

Kim et al, Nano Lett (2016)

θ=1.05

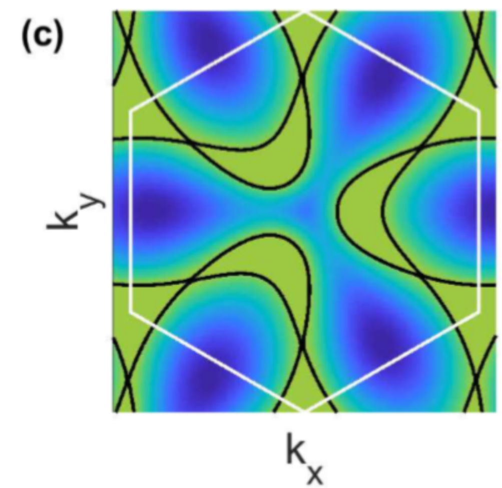

- 6 VHS away from ΓM line

Koshino et al Phys. Rev. X (2018)

Two VHS Configurations

θ=1.8 → θ=1.05

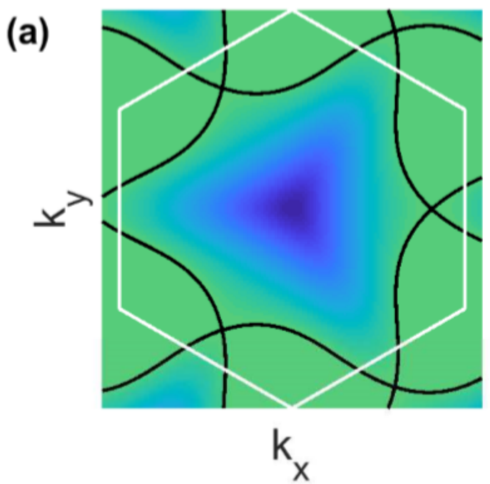

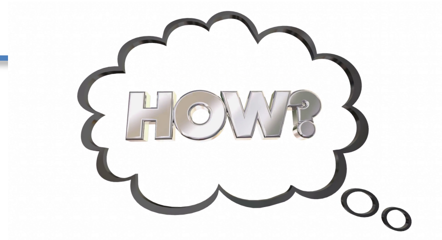

does one VHS configuration transition into the other as a function of twist angle?

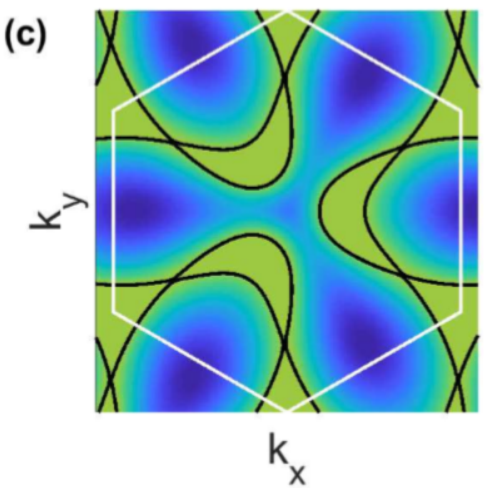

- 3 VHS on ΓM line
- 6 VHS away from ΓM line

When van Hove becomes *critical*

Yuan, Isobe & LF, arXiv:1901.05432

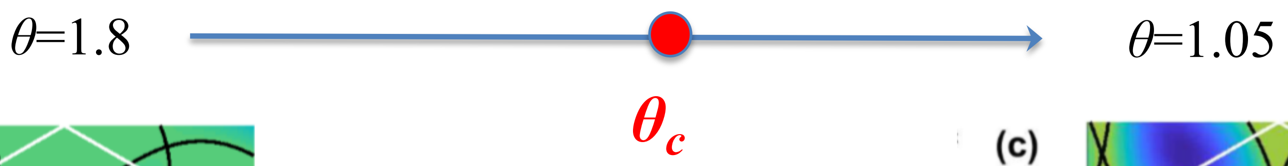

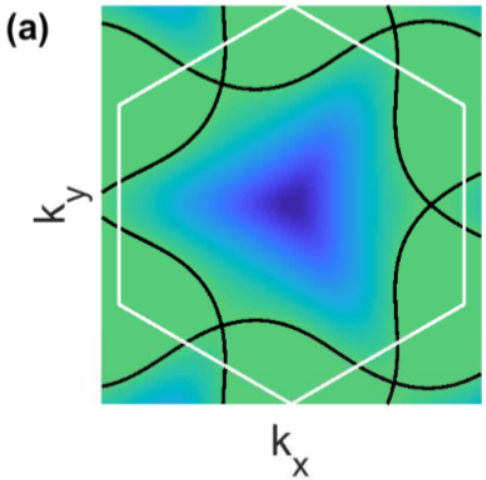

Splitting of one VHS on ΓM line into two on opposite sides

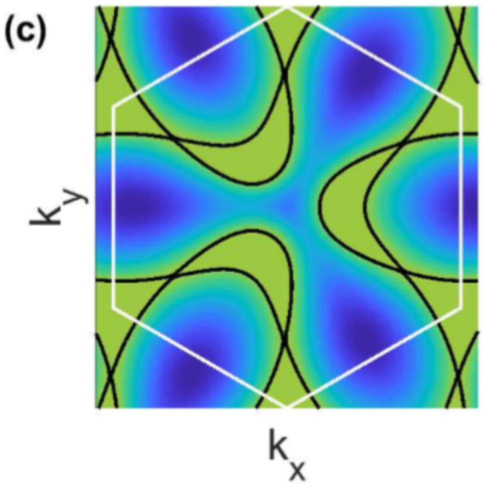

- 3 VHS on ΓM line
- 6 VHS away from ΓM line

High-Order Van Hove Singularity

θ=1.8 → θ=1.05

$\boldsymbol{\theta_c}$

Expansion around VHS on ΓM:

$$E - E_{\rm v} = -\alpha p_x^2 + \beta p_y^2 + \gamma p_x p_y^2 + \ldots$$

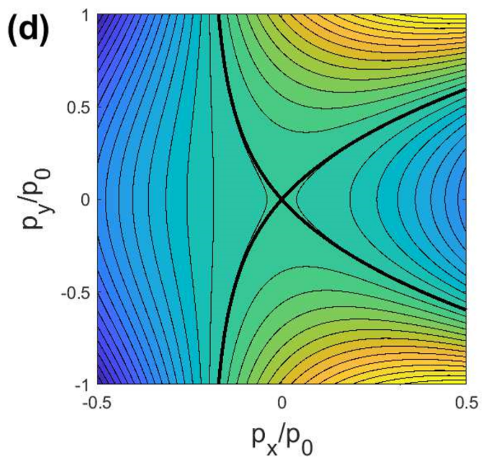

$\boldsymbol{\beta > 0}$**: VHS at** $\boldsymbol{p = 0}$

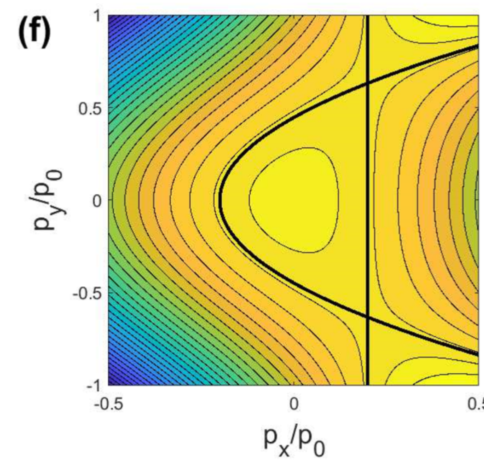

$\boldsymbol{\beta < 0}$**: two VHS at**

$$\Lambda_\pm = (-\beta/\gamma, \pm\sqrt{-2\alpha\beta}/\gamma)$$

High-Order Van Hove Singularity

θ=1.8 → θ_c → θ=1.05

$$E - E_{\rm v} = -\alpha p_x^2 + \beta p_y^2 + \gamma p_x p_y^2 + \ldots$$

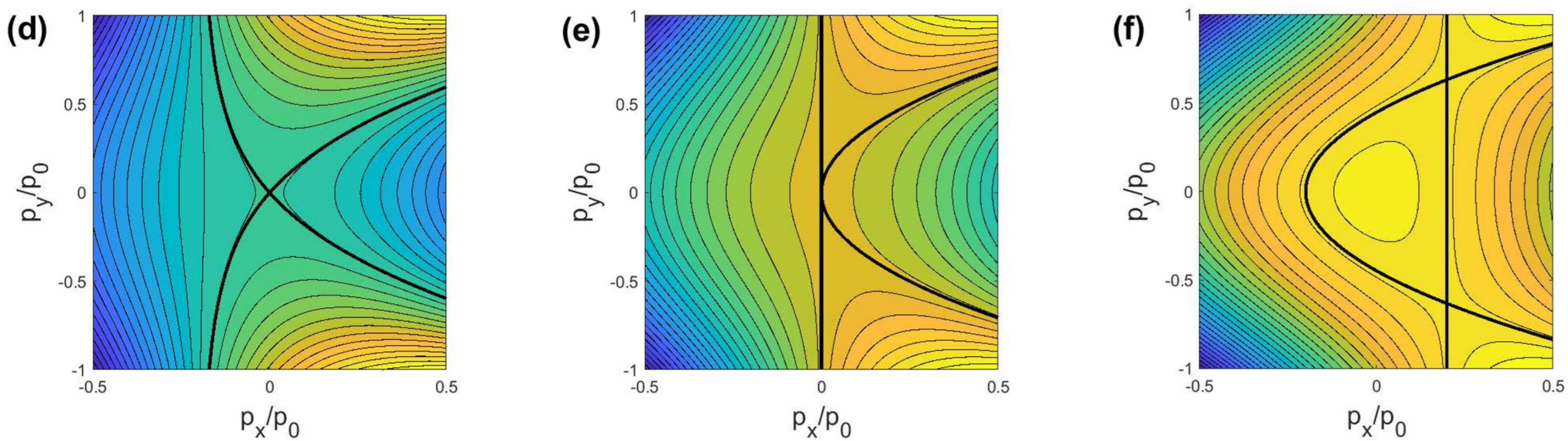

$\beta > 0$: VHS at $p = 0$

$\beta = 0$

$\beta < 0$: two VHS at

$$\Lambda_{\pm} = (-\beta/\gamma, \pm\sqrt{-2\alpha\beta}/\gamma)$$

High-Order Van Hove Singularity

θ=1.8 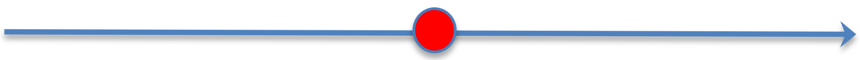 θ=1.05

$\boldsymbol{\theta_c}$

$$E - E_{\mathrm{v}} = -\alpha p_x^2 + \beta p_y^2 + \gamma p_x p_y^2 + \dots$$

$\boldsymbol{\beta = 0}$

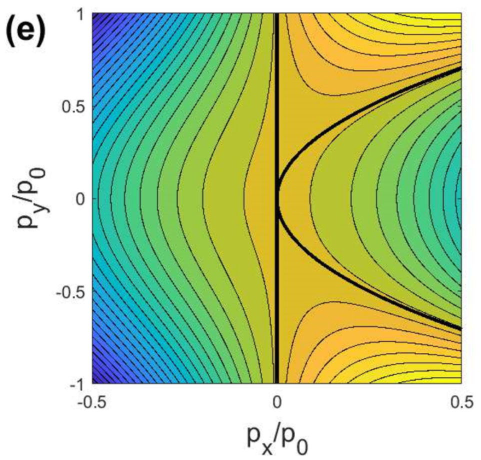

- two Fermi contours touch tangentially
- appear generally under tuning band structure with a **single parameter**, such as twist angle, pressure, electric field, strain…

High-Order Van Hove Singularity

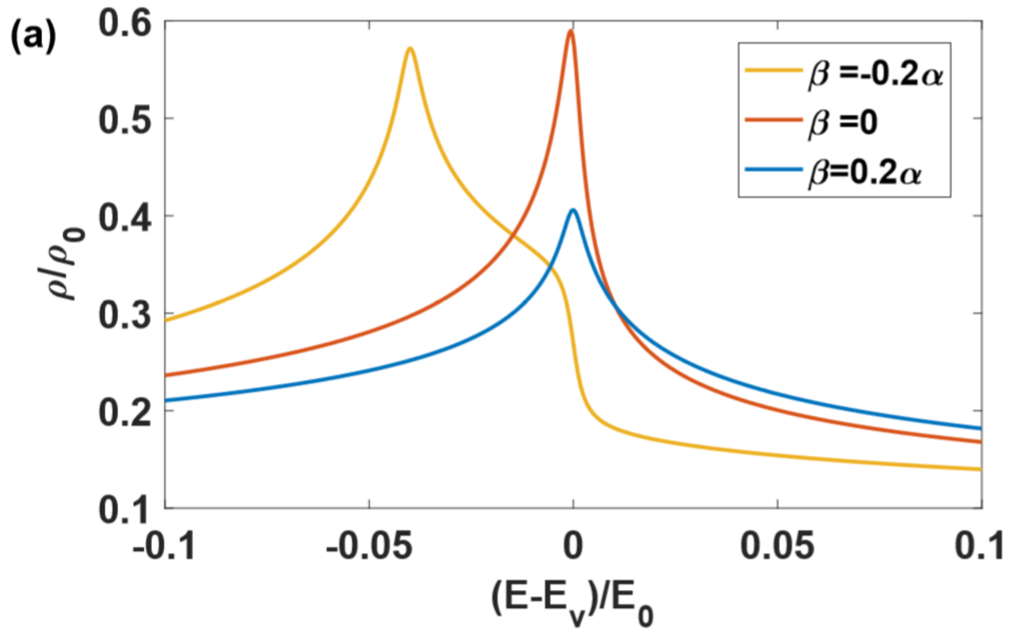

$\boldsymbol{\beta = 0}$:

$$\rho(E) = \frac{C}{\sqrt[4]{4\alpha\gamma^2}} \times \begin{cases} (E - E_{\mathrm{v}})^{-\frac{1}{4}} & E > E_{\mathrm{v}} \\ \sqrt{2}(E_{\mathrm{v}} - E)^{-\frac{1}{4}} & E < E_{\mathrm{v}} \end{cases} \qquad C = (2\pi)^{-\frac{5}{2}}\Gamma(\tfrac{1}{4})^2$$

- Power-law, instead of logarithmic, divergence.
- Distinctive peak asymmetry

High-Order Van Hove Singularity

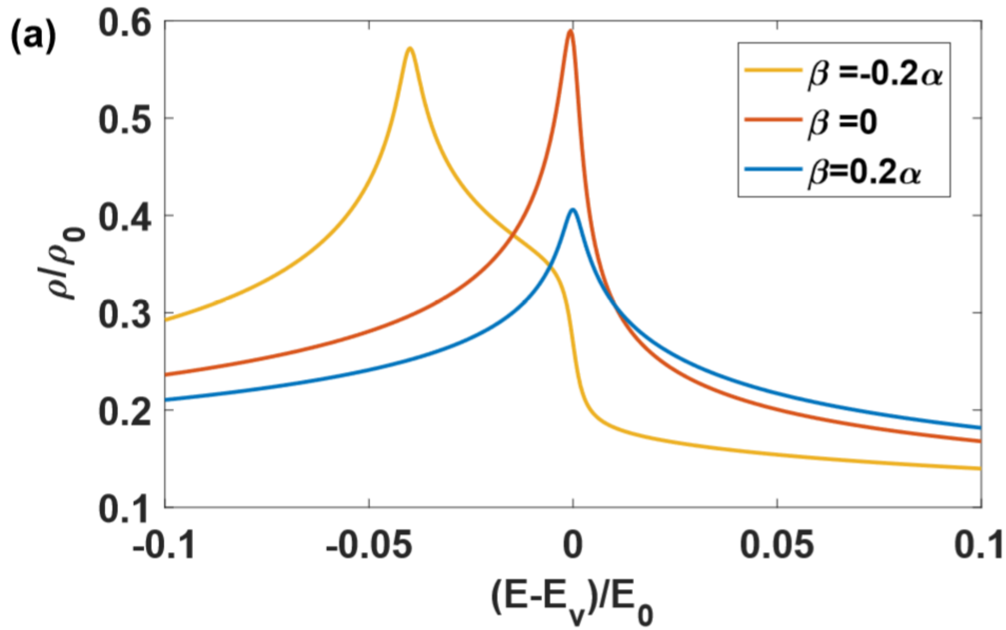

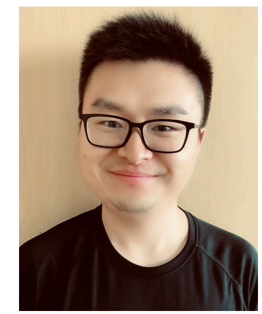

General $\boldsymbol{\beta}$:

$$\rho(E) = \frac{\mathrm{sgn}(r)}{\sqrt{2}\alpha\pi^2}\left[\mathrm{Re} f(\varepsilon, r) + \mathrm{Im} g(\varepsilon, r)\Theta(-r)\right] \qquad r = \beta/\alpha$$

$$z_\pm = r \pm \sqrt{r^2 + \varepsilon}.$$

$$f(\varepsilon, r) = \frac{1}{\sqrt{z_-}}\mathrm{K}\left(1 - \frac{z_+}{z_-}\right), \quad g(\varepsilon, r) = \frac{2}{\sqrt{z_+}}\mathrm{K}\left(\frac{z_-}{z_+}\right)$$

complete elliptic integral of the first kind

STM

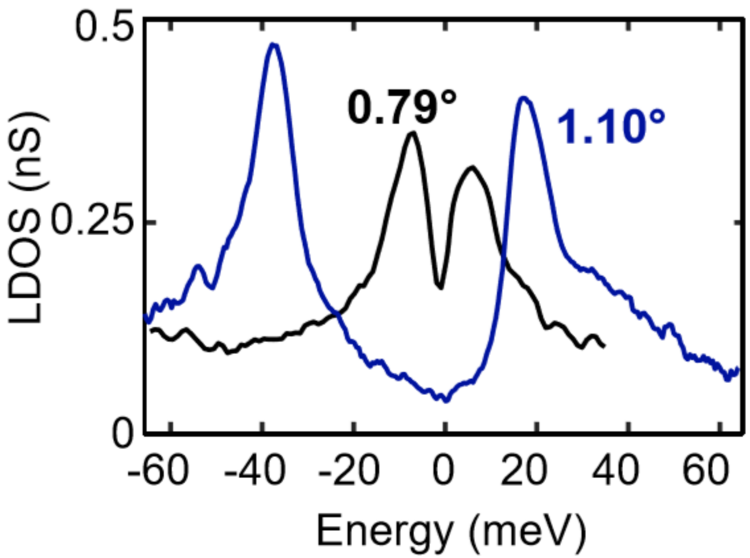

October 2018

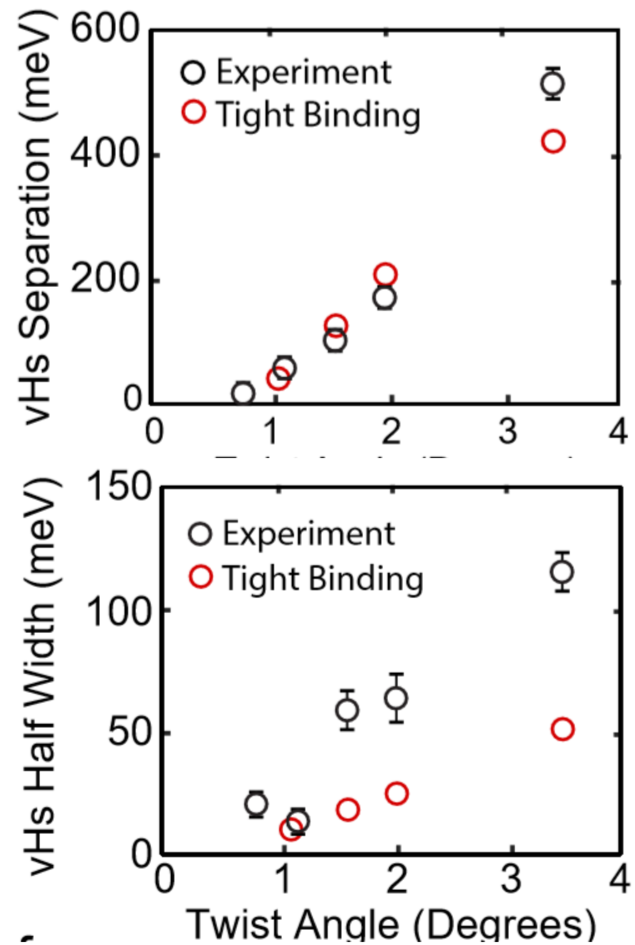

Pasupathy & Dean, arXiv:1812.08776

Fitting with High-Order VHS

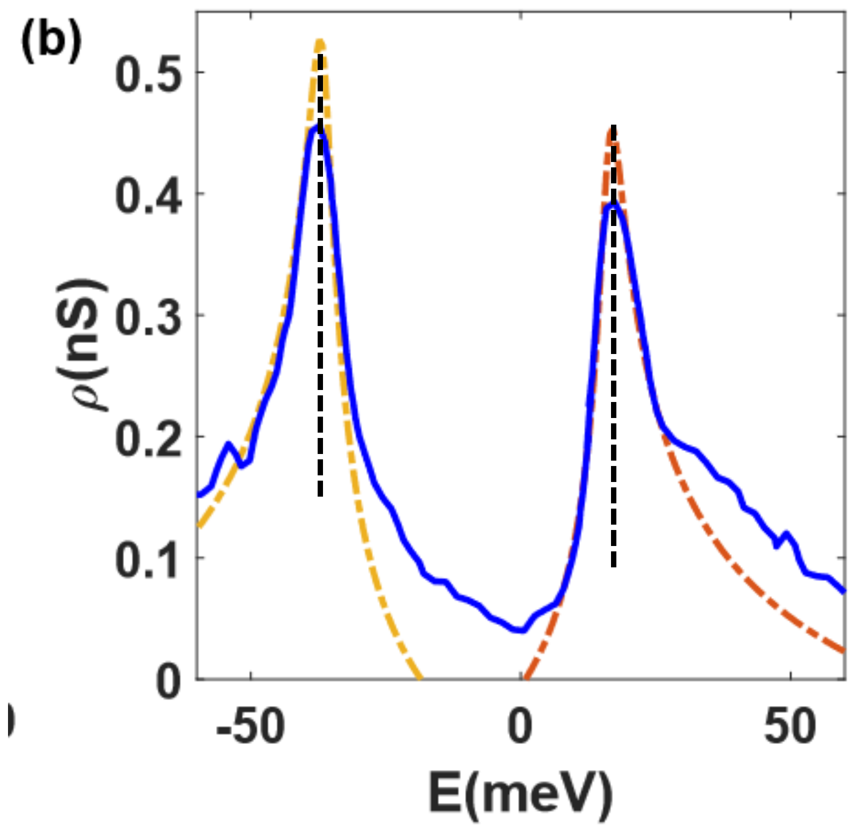

STM Data (blue) provided by Abhay Pasupathy and Alex Kerelsky

Many-Body Splitting at VHS

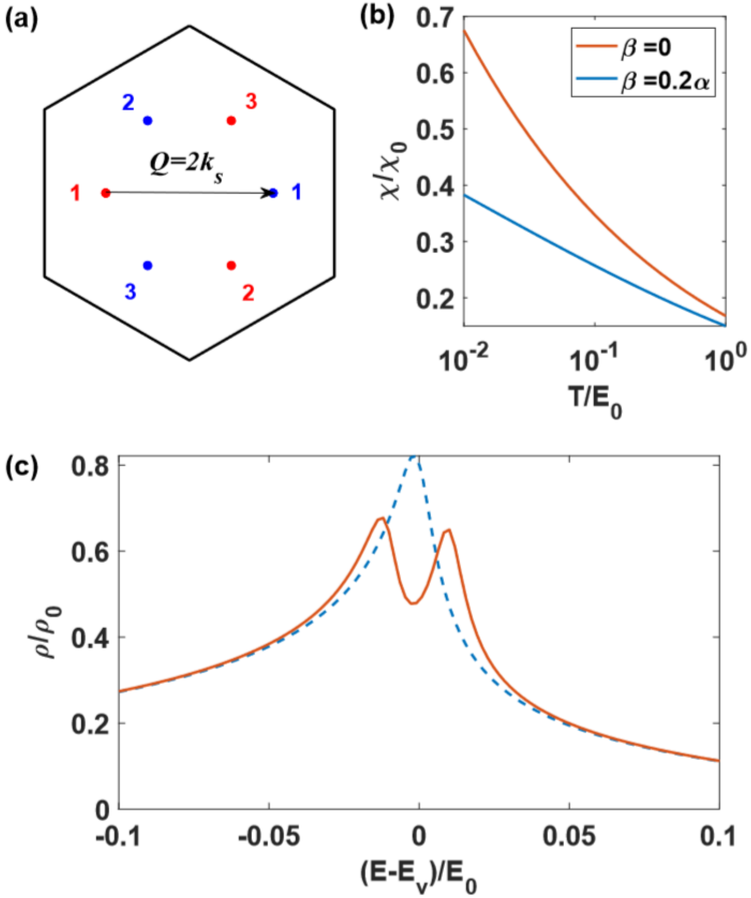

At high-order VHS,

- Perfect nesting leads to bare susceptibility growing faster than log(1/T)
- splitting of VHS peak due to broken symmetry: density wave, nematicity etc

Tuning to Magic Van Hove Singularity

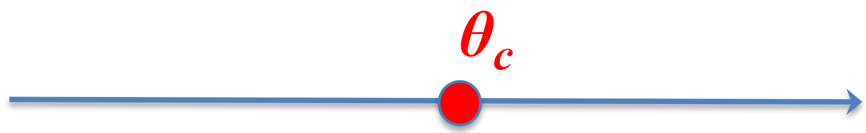

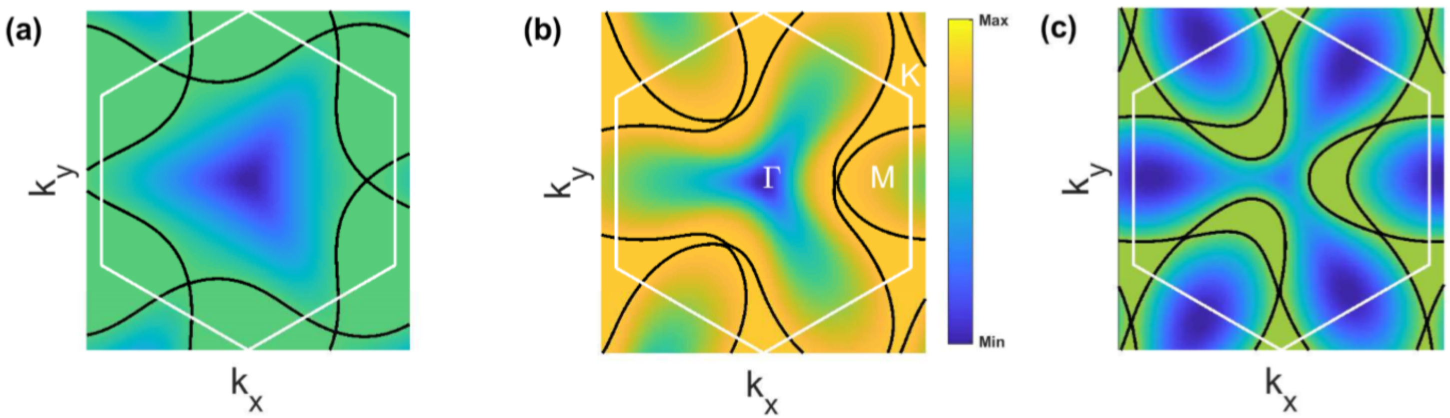

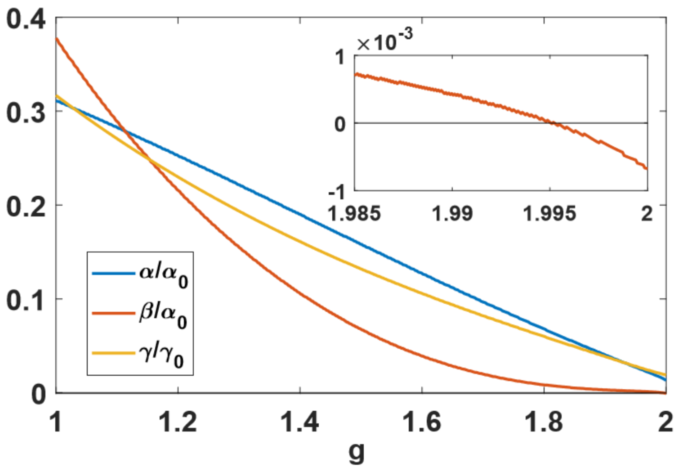

For v/a = 2.41eV, 13% larger than DFT value and u = 79.7meV, u' = 97.5meV, θ_c = 0.95.

$\theta_{\rm exp} \in [1^\circ, 1.2^\circ]$ ⟺ $g_{\rm exp} \in [1.6, 1.9]$

where VHS is close to high-order ($\beta \ll \alpha, \gamma$) and half-filling.

Tuning to High-Order VHS in Moire Materials

1. Creating electron correlation by tuning single-particle dispersion at VHS (with electric field, pressure, strain)
2. Gating to van Hove filling

Open questions about high-order VHS:

- Symmetry-based classification
- T-dependence of scattering rate & resistivity
- Competing states

…

Effective Tight-Binding and Hubbard Model

First Step towards Strong Coupling

Our approach:

Wannier orbital in real space must match band symmetry in k space

Band Structure

↓

Band Symmetry at high symmetry points

↓

Centers and Symmetry of Wannier Orbitals

↓

Wannier Orbitals

↓

Tight-Binding Model

Wannier orbitals are defined for commensurate lattice systems, <u>NOT for continuum model</u>!

Envelop Function * Bloch Phase Factor

from continuum model   from underlying lattice

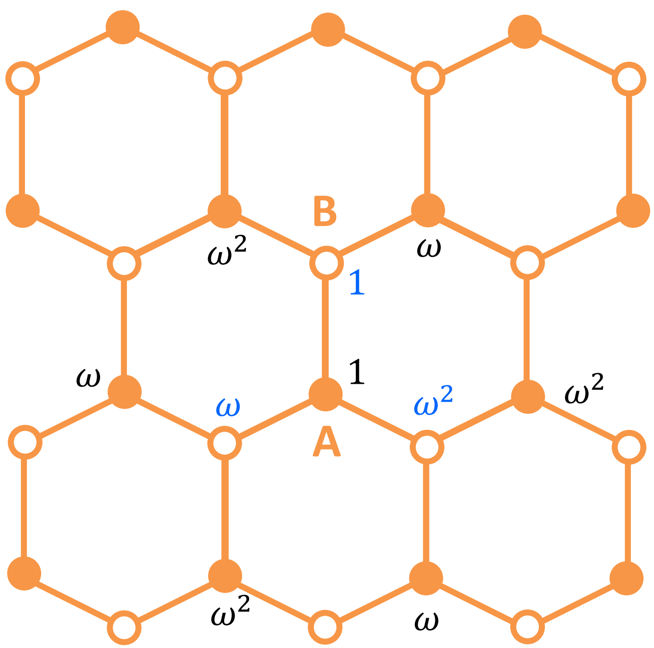

$\omega = e^{2i\pi/3} = \exp(iK \cdot R)$

At +/-***K*** point, the Bloch wave functions of A, B sites will assign different phases to different sites.

With respect to rotation center of C_{3z} at A site, Bloch states at A sites have $L_z = 0$.

Bloch states at B sites have $L_z = 1$ at +K and $L_z = -1$ at -K

k-Space to r-Space

	Γ	K	M
Group	D_3	D_3	C_2
Reps	$\{E, E\}$	$\{A_1, A_2, E\}$	$\{A, A, B, B\}$

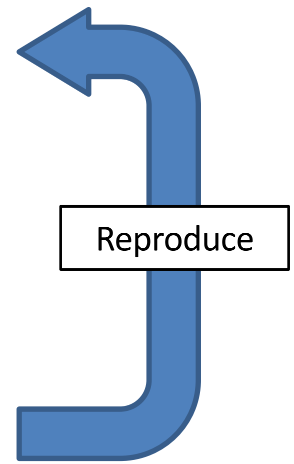

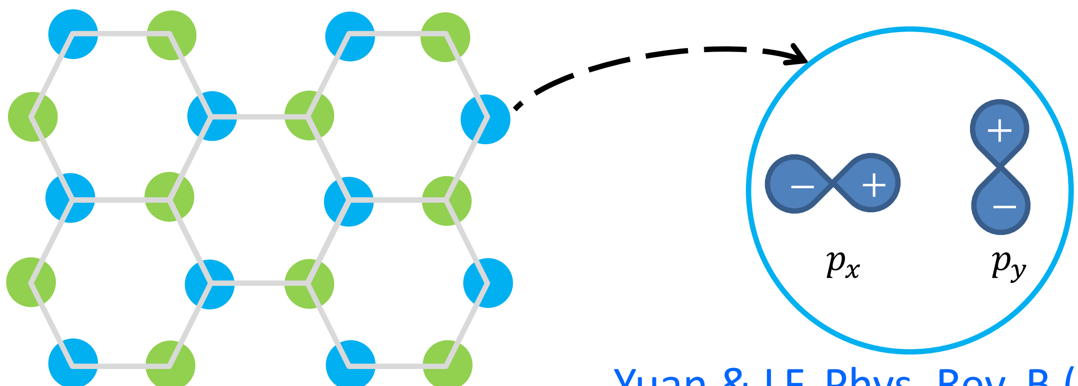

Yuan & LF, Phys. Rev. B (2018)
See also Jiang & Vafek, Phys. Rev. X (2018)

- Wannier orbitals centered at AB and BA region form a honeycomb lattice.
- A doublet of Wannier orbitals with $p_x \pm ip_y$ on-site symmetry, originating from K and K' valley respectively.

Wannier functions: three-peak structure & $p_x \pm ip_y$ symmetry

Orbital 1 (A-like): AB-centered

Koshino, Yuan et al, Phys. Rev. X (2018)

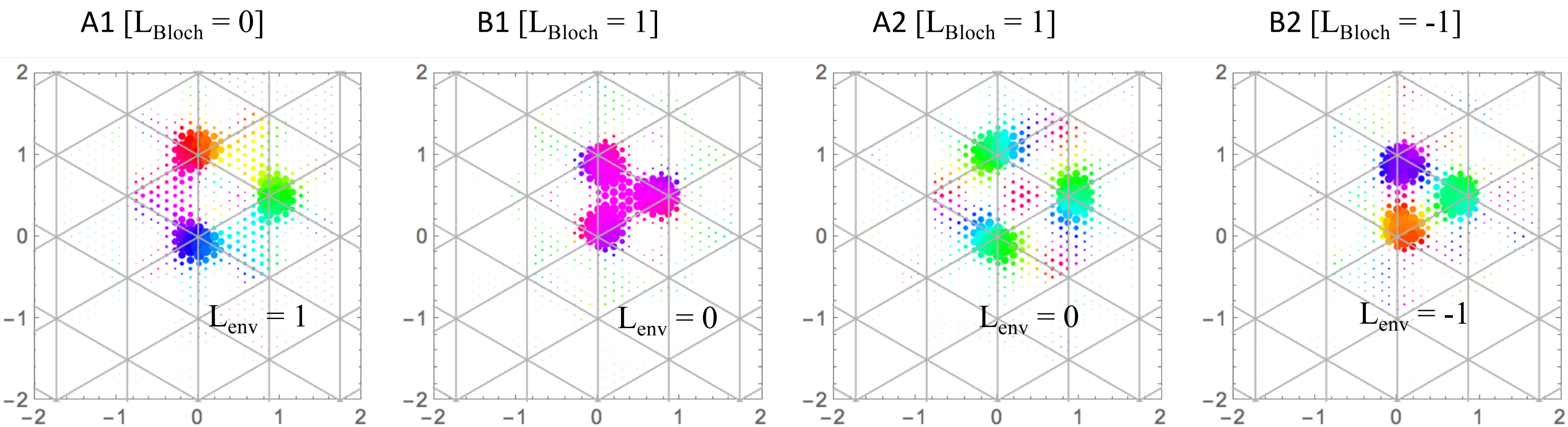

Orbital 2 (B-like) : BA-centered

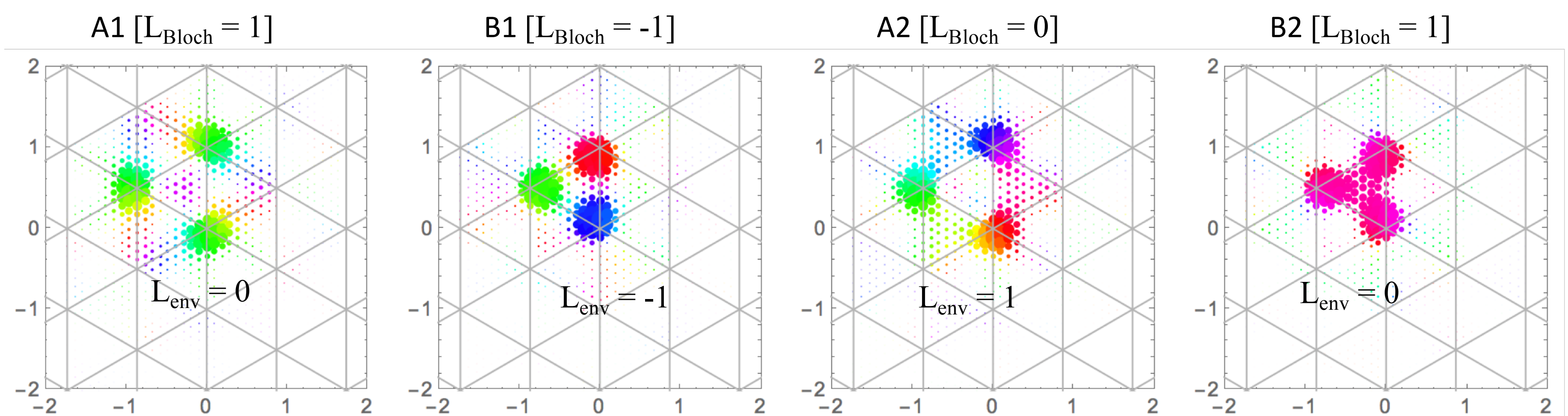

Effective TB Model

Hamiltonian in Wannier orbital basis
(NOT FITTING)

Dominant hoppings:
t_1, t_5 & it_2 (imaginary)

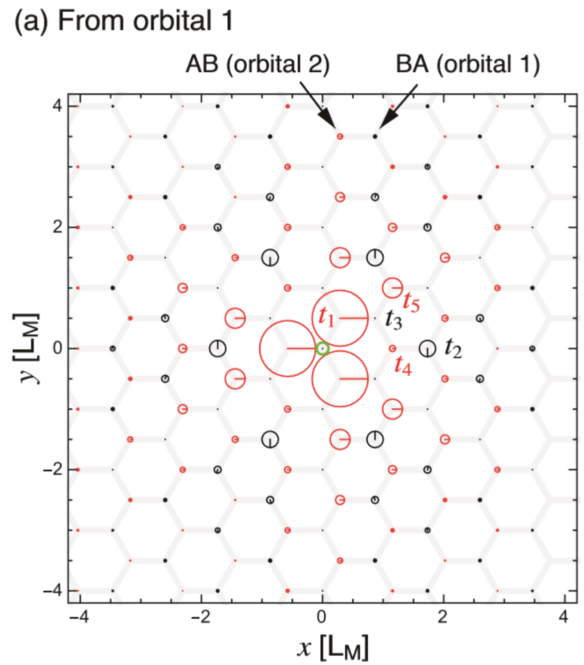

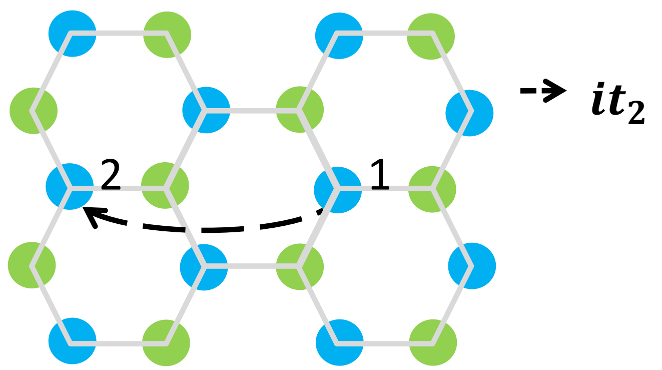

Symmetry in our TB Model for single valley:
C_3 & $C_{2x}, C_{2z}T$

Koshino, Yuan, Koretsune, Ochi, Kuroki & LF, PRX (2018)

See also Jiang & Vafek, Phys. Rev. X (2018)

Extended Hubbard Model

Koshino et al, PRX (2018)

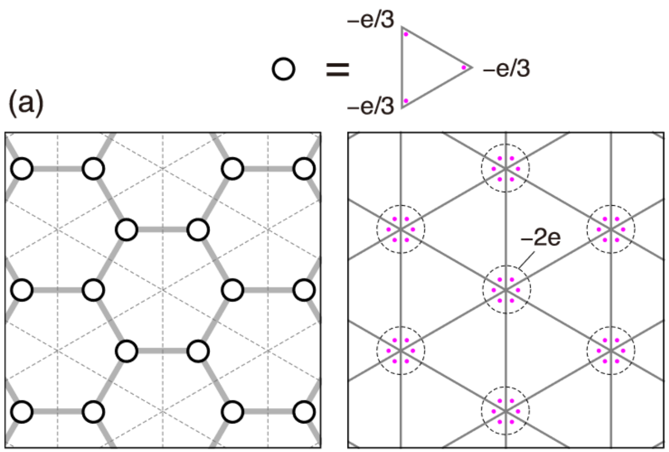

TABLE I. Direct interaction V_n and the exchange interaction J_n for the Wannier orbitals in units of $e^2/(\epsilon L_{\mathrm{M}})$. The definition of $V_0, V_1 \cdots$ is presented in Fig. 6(a). $V_n^{(\mathrm{approx})}$ is the direct interaction terms estimated by the point-charge approximation (see the text).

n	0	1	2	3	4	5
V_n	1.857	1.533	1.145	1.068	0.697	0.614
$V_n^{(\mathrm{approx})}$	1.857	1.524	1.136	1.081	0.679	0.610
J_n	N/A	0.376	0.0645	0.010	0.014	0.001

see also Po et al, PRX (2018); Jiang & Vafek

Models with more bands:

Hejazi, Liu, Shapourian, Chen, Balents,
Po, Zou, Senthil, Vishwanath,
Chen, Bernevig,
Fang, Carr, Kaxiras …

Two-Orbital Honeycomb Hubbard Model

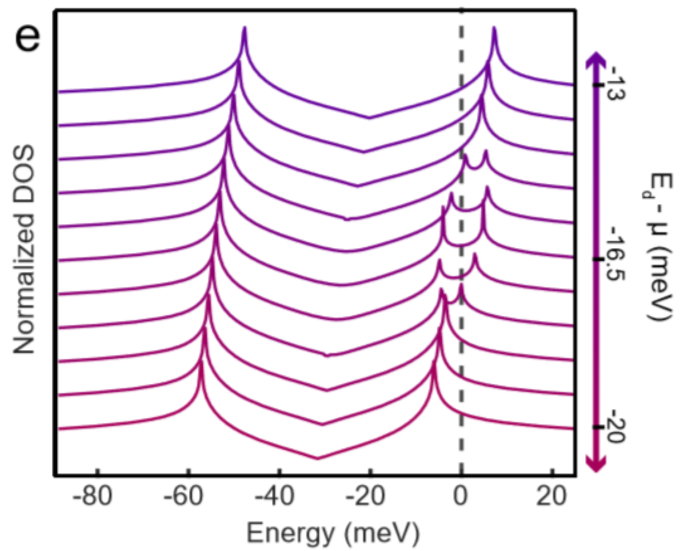

Pasupathy & Dean: **arXiv:1812.08776**

Extended interaction leads to Fock term renormalizes TB hopping
=> Bandwidth is filling-dependent
(no symmetry breaking at charge neutrality)

See also Paco Guinea (PNAS, 2018)

Summary

- Narrow moire band and van Hove singularity
- Unconventional SC and density wave near VHS
- Tuning to **magic VHS**
- Effective tight-binding/Hubbard model